Supplementary Materials for Interdecadal variations in the Walker circulation and its connection to inhomogeneous air temperature changes during 1961–2012

Xiaoya Hou [1], Jianbo Cheng [1], Shujuan Hu [1,*], Guolin Feng [2]

[1] Key Laboratory of Semi-Arid Climate Change of Ministry of Education, College of Atmospheric Sciences, Lanzhou University, Lanzhou 730000, China

[2] Physical Science and Technology College of Yangzhou University, Yangzhou 225002, China

***** Correspondence: hushuju@lzu.edu.cn; Tel.: +86-13309400827

Contents of this file

Figure S1 a Mean state (1961–2012) of the annual mean meridionally averaged air temperature (K) between 5°S and 5°N using the JRA-55 reanalysis dataset. **b** homogeneous part of **a** (global zonal mean of **a**). **c** inhomogeneous part of **a** (**a** minus **b**).

Figure S2 a Mean state (1961–2012) of the annual mean meridionally averaged ZSF (10^{-6} s^{-1}) between 5°S and 5°N using the JRA-55 reanalysis dataset. **b** homogeneous part of **a** (global zonal mean of **a**). **c** inhomogeneous part of **a** (**a** minus **b**).

Figure S3 Contours in **a** and **b**: mean state (1961–2012) of the annual mean zonal circulations along the equator (5°S–5°N); shading: differences in the annual mean zonal circulations between **a** the periods 1961–1974 and 1977–1997 and **b** the periods 1977–1997 and 1999–2012. The changes statistically significant at the 5% confidence level are dotted in purple. The zonal circulations are represented by the MSF (10^{11} kg s^{-1}) derived from the method developed by Schwendike et al. [1,2].

Figure S4 Same as Figure S3 but for the mean state (contours) of and differences (shading) in the monthly mean of vertically averaged zonal circulations. The zonal circulations are represented by the MSF (10^{11} kg s^{-1}) derived from the method developed by Schwendike et al. [1,2].

Figure S5 Differences in the zonal circulation (contours; 10^{11} kg s^{-1}) and inhomogeneous air temperature (shading; K) along the equator (5°S–5°N) between **a** El Niño and La Niña, **b** La Niña and El Niño, **c** the periods 1961–1974 and 1977–1997, and **d** the periods 1977–1997 and 1999–2012. The zonal circulations are represented by the MSF derived from the method developed by Schwendike et al. [1,2].

Figure S6 Time series (1961–2012) of the normalized annual mean tropical PWC intensity indices based on the SLP (defined as the mean SLP over the region (5°S–5°N, 80°W–160°W) minus the mean SLP over the region (5°S–5°N, 80°E–160°E); black line), air temperature (defined as in Equation (13) in the main text; blue line), and MSF (defined as the mean value of the MSF over the region (5°S–5°N, 140°W–180°, 300–600 hPa); red line)

Figure S7 Spatial pattern of the regressed **a** SST (K), **b** SLP (hPa), **c** zonal winds of the zonal circulation at 1000 hPa (m s^{-1}), and **d** precipitation (mm d^{-1}) against the normalized PWC intensity index based on the MSF for the period 1961–2012. The regression coefficients statistically significant at the 5% confidence level are dotted in black.

Introduction

We provide figures in the Supplementary Materials to support the results discussed in the main text. Figures S1 and S2 serve as examples for the explanation of the "inhomogeneous" concept proposed in the main text. Figures S3–S7 display the results that are the interdecadal variations in the PWC and its connection to inhomogeneous air temperature changes by using the mass stream function (MSF) derived from the method proposed by Schwendike et al. [1,2]. Figures S3–S7 support the comparison of the method proposed by Schwendike et al. [1,2] and the three-pattern decomposition of global atmospheric circulation (3P-DGAC) method [3,4] in representing the PWC.

In addition, in the Supplementary Materials, we provide an explanation of the "inhomogeneous" concept proposed in the main text, a brief description of the method proposed by Schwendike et al. [1,2] (i.e., the local partitioning method of the overturning circulation in the tropics), and a brief introduction of the new dynamical equations derived from the 3P-DGAC method [3,4].

Explanation of the "inhomogeneous" concept proposed in the main text

In this section, we give an explanation of the "inhomogeneous" concept proposed in the main text. In this paper, the "homogeneous" part of one variable is defined as the global zonal mean of the variable, and the "inhomogeneous" part of the variable is defined as the difference between the variable and the "homogeneous" part of the variable (i.e., the variable minus the global zonal mean of the variable). Figures S1 and S2 are two examples that can be used to explain the "inhomogeneous" concept. Figures

S1a–c display the mean state of the annual mean meridionally averaged air temperature between 5 °S and 5 °N, the “homogeneous” part of the air temperature, and the “inhomogeneous” part of the air temperature, respectively. Figures S2a–c display the mean state of the annual mean meridionally averaged zonal stream function (ZSF) between 5 °S and 5 °N, the “homogeneous” part of the ZSF, and the “inhomogeneous” part of the ZSF, respectively. Thus, the “inhomogeneous air temperature” in the main text is the difference between the air temperature and the global zonal mean of the air temperature.

Local partitioning method of the overturning circulation in the tropics (see also Schwendike et al. [1,2])

According to Schwendike et al. [1,2], the horizontal vortex circulation $\vec{V}_{rot} = u_{rot}\vec{i} + v_{rot}\vec{j}$ at low latitudes that satisfies

$$\nabla_p \cdot \vec{V}_{rot} = \frac{1}{a\cos\varphi}\frac{\partial u_{rot}}{\partial \lambda} + \frac{1}{a\cos\varphi}\frac{\partial v_{rot}\cos\varphi}{\partial \varphi} = 0, \tag{S1}$$

is often neglected. Thus, the large-scale motion in the low latitudes is represented as follows:

$$\vec{V} = \vec{V}_{div} + \omega\vec{k}, \tag{S2}$$

which satisfies the continuity equation as follows:

$$\nabla_p \cdot \vec{V}_{div} + \frac{\partial \omega}{\partial p} = \frac{1}{a\cos\varphi}\frac{\partial u_{div}}{\partial \lambda} + \frac{1}{a\cos\varphi}\frac{\partial v_{div}\cos\varphi}{\partial \varphi} + \frac{\partial \omega}{\partial p} = 0. \tag{S3}$$

By using Equations (S2) and (S3), Schwendike et al. [1,2] defined the zonal overturning circulation $\vec{V}_{\lambda}$ and the meridional overturning circulation $\vec{V}_{\varphi}$ in the tropics as follows:

$$\vec{V}_\lambda = u_{div}\vec{i} + \omega_\lambda \vec{k}, \quad \vec{V}_\varphi = v_{div}\vec{i} + \omega_\varphi \vec{k}, \tag{S4}$$

which satisfy the following continuity equations:

$$\frac{1}{a\cos\varphi}\frac{\partial u_{div}}{\partial \lambda} + \frac{\partial \omega_\lambda}{\partial p} = 0, \tag{S5}$$

$$\frac{1}{a\cos\varphi}\frac{\partial v_{div}\cos\varphi}{\partial \varphi} + \frac{\partial \omega_\varphi}{\partial p} = 0. \tag{S6}$$

Equations (S5) and (S6) ensure that the components u_{div}, ω_λ, v_{div}, and ω_φ can be represented by the stream functions ψ_λ and ψ_φ as follows:

$$u_{div} = -\frac{\partial \psi_\lambda}{\partial p}, \quad \omega_\lambda = \frac{1}{a\cos\varphi}\frac{\partial \psi_\lambda}{\partial \lambda}, \tag{S7}$$

$$v_{div} = -\frac{\partial \psi_\varphi}{\partial p}, \quad \omega_\varphi = \frac{1}{a\cos\varphi}\frac{\partial \psi_\varphi \cos\varphi}{\partial \varphi}. \tag{S8}$$

Equations (S2), (S4), (S5), and (S6) can be combined to generate the following:

$$\vec{V} = \vec{V}_{div} + \omega\vec{k} = \vec{V}_\lambda + \vec{V}_\varphi, \tag{S9}$$

which means that $\vec{V}_\lambda$ and $\vec{V}_\varphi$ represent a decomposition of the overturning circulation at low latitudes. In addition, Equations (S5) and (S6) also represent a decomposition of the continuity equation (S3). Schwendike et al. [1,2] referred to Equation (S9) as the local partitioning of the overturning circulation in the tropics and $\vec{V}_\lambda$ and $\vec{V}_\varphi$ as the local Hadley and Walker circulations, respectively.

In the summary section of the main text, the zonal velocity u_{div} and mass stream function (MSF) $MSF = \frac{\pi a}{g}\int_p^0 u_{div}\,dp$ (p is pressure, a is the earth's radius, and g is the gravitational acceleration) of the local Walker circulation are used. Additional details of the local partitioning method can be obtained from Schwendike et al. [1,2].

New dynamical equations derived from the 3P-DGAC method (see also Hu et al. [3,4])

The new dynamical equations of the horizontal, meridional, and zonal circulations can be obtained by combining the three-pattern decomposition of global atmospheric circulation (3P-DGAC) method and the primary equations as follows:

$$\frac{\partial}{\partial t}\left(-\frac{\partial^2 H}{\partial \sigma^2}+\frac{1}{\sin\theta}\frac{\partial^2 R}{\partial\lambda\partial\sigma}\right)-\frac{\partial}{\partial\sigma}\pi'\frac{\partial H}{\partial\sigma}-\frac{\partial}{\partial\sigma}A'\frac{\partial W}{\partial\sigma}+\frac{\partial}{\partial\sigma}\left(A'\frac{\partial R}{\partial\theta}+\pi'\frac{1}{\sin\theta}\frac{\partial R}{\partial\lambda}\right)$$

$$+\frac{\partial}{a\partial\sigma}\tilde{L}_1'\left(\frac{1}{\sin\theta}\frac{\partial R}{\partial\lambda}-\frac{\partial H}{\partial\sigma}\right)=\frac{R_0}{a^2\sigma}\frac{\partial T}{\partial\theta}, \qquad \text{(S10)}$$

$$\frac{\partial}{\partial t}\left(\frac{\partial^2 W}{\partial \sigma^2}-\frac{\partial^2 R}{\partial\theta\partial\sigma}\right)-\frac{\partial}{\partial\sigma}A'\frac{\partial H}{\partial\sigma}+\frac{\partial}{\partial\sigma}\pi'\frac{\partial W}{\partial\sigma}+\frac{\partial}{\partial\sigma}\left(A'\frac{1}{\sin\theta}\frac{\partial R}{\partial\lambda}-\pi'\frac{\partial R}{\partial\theta}\right)$$

$$+\frac{\partial}{a\partial\sigma}\tilde{L}_1'\left(\frac{\partial W}{\partial\sigma}-\frac{\partial R}{\partial\theta}\right)=\frac{R_0}{a^2\sigma}\frac{1}{\sin\theta}\frac{\partial T}{\partial\lambda}, \qquad \text{(S11)}$$

$$\frac{\partial}{\partial t}(\Delta_3 R)+\frac{1}{\sin\theta}\left(\frac{\partial}{\partial\theta}\sin\theta A'\frac{\partial H}{\partial\sigma}-\frac{\partial}{\partial\lambda}\pi'\frac{\partial H}{\partial\sigma}\right)-\frac{1}{\sin\theta}\left(\frac{\partial}{\partial\theta}\sin\theta\pi'\frac{\partial W}{\partial\sigma}+\frac{\partial}{\partial\lambda}A'\frac{\partial W}{\partial\sigma}\right)$$

$$+\frac{1}{\sin\theta}\left(\frac{\partial}{\partial\theta}\sin\theta\pi'\frac{\partial R}{\partial\theta}+\frac{\partial}{\partial\lambda}\pi'\frac{1}{\sin\theta}\frac{\partial R}{\partial\lambda}-\frac{\partial}{\partial\theta}A'\frac{\partial R}{\partial\lambda}+\frac{\partial}{\partial\lambda}A'\frac{\partial R}{\partial\theta}\right)$$

$$+\frac{1}{a\sin\theta}\frac{\partial}{\partial\lambda}\tilde{L}_1'\left(\frac{1}{\sin\theta}\frac{\partial R}{\partial\lambda}-\frac{\partial H}{\partial\sigma}\right)-\frac{1}{a\sin\theta}\frac{\partial}{\partial\theta}\sin\theta\tilde{L}_1'\left(\frac{\partial W}{\partial\sigma}-\frac{\partial R}{\partial\theta}\right)=0, \qquad \text{(S12)}$$

$$\frac{R_0^2}{ac^2}\frac{\partial T}{\partial t}-\frac{R_0}{a\sigma}\left(\frac{1}{\sin\theta}\frac{\partial(\sin\theta H)}{\partial\theta}-\frac{1}{\sin\theta}\frac{\partial W}{\partial\lambda}\right)+\frac{R_0^2}{ac^2}\pi'T+\tilde{L}_2'T=\frac{R_0^2}{ac^2}\frac{\varepsilon}{c_p}, \qquad \text{(S13)}$$

where R, H, and W represent the stream functions of the horizontal, meridional, and zonal circulations, respectively. $\pi'=\frac{u'}{\sin\theta}\frac{\partial}{\partial\lambda}+v'\frac{\partial}{\partial\theta}+\dot{\sigma}\frac{\partial}{\partial\sigma}$, $A'=2\Omega\cos\theta+ctg\theta u'$, $c^2=\frac{R_0^2\overline{T}}{g}(\gamma_d-\overline{\gamma})$, $\tilde{L}_1'=-a\frac{\partial}{\partial\sigma}\nu_1\left(\frac{g\sigma}{R_0\overline{T}}\right)^2\frac{\partial}{\partial\sigma}-a\mu_1\nabla^2$, $\tilde{L}_2'=-\frac{1}{a}\frac{\partial}{\partial\sigma}\nu_2\left(\frac{g\sigma}{R_0\overline{T}}\right)^2\frac{\partial}{\partial\sigma}-\frac{1}{a}\mu_2\nabla^2$, and $\nabla^2=\frac{1}{a^2\sin^2\theta}\frac{\partial^2}{\partial\lambda^2}+\frac{1}{a^2\sin\theta}\frac{\partial}{\partial\theta}\sin\theta\frac{\partial}{\partial\theta}$.

A simplified model of the new dynamical equations can be obtained as follows:

$$\frac{\partial}{\partial t}\left(-\frac{\partial^2 H}{\partial \sigma^2}+\frac{1}{\sin\theta}\frac{\partial^2 R}{\partial\lambda\partial\sigma}\right)=\frac{R_0}{a^2\sigma}\frac{\partial T}{\partial\theta}, \qquad \text{(S14)}$$

$$\frac{\partial}{\partial t}\left(\frac{\partial^2 W}{\partial \sigma^2} - \frac{\partial^2 R}{\partial \theta \partial \sigma}\right) = \frac{R_0}{a^2 \sigma} \frac{1}{\sin\theta} \frac{\partial T}{\partial \lambda}, \quad \text{(S15)}$$

$$\frac{\partial}{\partial t}(\Delta_3 R) = -\pi_R'(\Delta_2 R - f), \quad \text{(S16)}$$

$$\frac{\partial}{\partial t}\left(\frac{R_0{}^2}{a^2 c^2} T\right) = \frac{R_0}{a^2 \sigma} \frac{1}{\sin\theta}\left(\frac{\partial}{\partial \theta}\sin\theta H - \frac{\partial W}{\partial \lambda}\right) - \frac{R_0{}^2}{a^2 c^2} \pi_R' T, \quad \text{(S17)}$$

where $\pi_R' = \frac{u_R'}{\sin\theta} \frac{\partial}{\partial \lambda} + v_R' \frac{\partial}{\partial \theta}$ and $\Delta_2 = \frac{1}{\sin^2\theta} \frac{\partial^2}{\partial \lambda^2} + \frac{1}{\sin\theta} \frac{\partial}{\partial \theta}(\sin\theta \frac{\partial}{\partial \theta})$.

More details on the new dynamical equations derived from the 3P-DGAC method and its simplified model can be obtained in Hu et al. [3,4].

References

1. Schwendike, J.; Govekar, P.; Reeder, M.J.; Wardle, R.; Berry, G.J.; Jakob, C. Local partitioning of the overturning circulation in the tropics and the connection to the Hadley and Walker circulations. J. Geophys. Res. **2014**, 119, 1322–1339. https://doi.org/10.1002/2013jd020742
2. Schwendike, J.; Berry, G.J.; Reeder, M.J.; Jakob, C.; Govekar, P.; Wardle, R. Trends in the local Hadley and local Walker circulations. J. Geophys. Res. **2015**, 120, 7599–7618. https://doi.org/10.1002/2014jd022652
3. Hu, S.; Chou, J.; Cheng, J. Three-pattern decomposition of global atmospheric circulation: Part I—Decomposition model and theorems. Clim. Dyn. **2018**, 50, 2355–2368. https://doi.org/10.1007/s00382-015-2818-4
4. Hu, S.; Cheng, J.; Xu, M.; Chou, J. Three-pattern decomposition of global atmospheric circulation: part II—dynamical equations of horizontal, meridional

and zonal circulations. Clim. Dyn. **2018**, 50, 2673–2686. https://doi.org/10.1007/s00382-017-3763-1

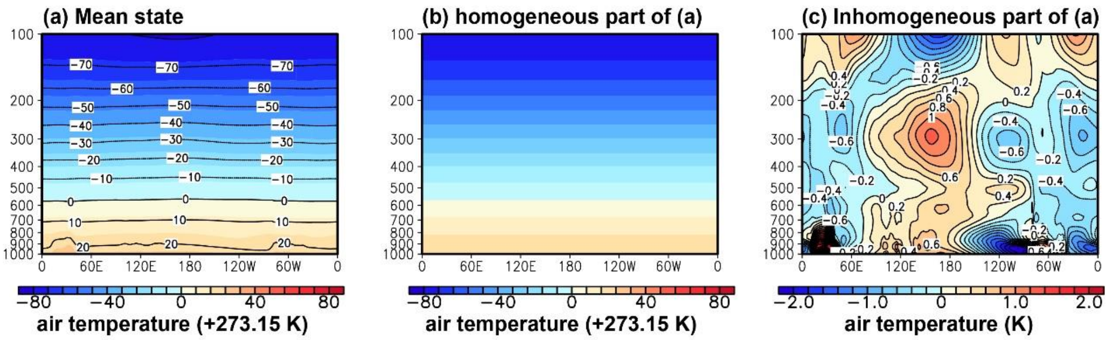

Figure S1 a Mean state (1961–2012) of the annual mean meridionally averaged air temperature (K) between 5°S and 5°N using the JRA-55 reanalysis dataset. **b** homogeneous part of **a** (global zonal mean of **a**). **c** inhomogeneous part of **a** (**a** minus **b**).

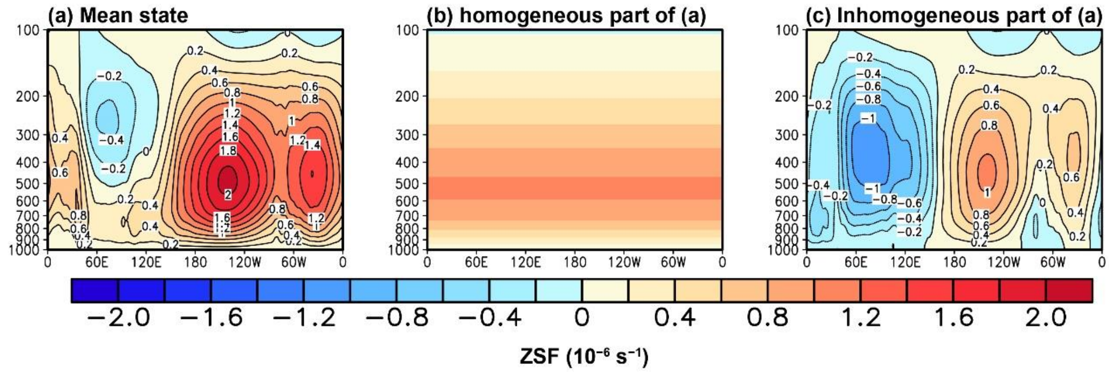

Figure S2 a Mean state (1961–2012) of the annual mean meridionally averaged ZSF (10^{-6} s^{-1}) between 5 °S and 5 °N using the JRA-55 reanalysis dataset. **b** homogeneous part of **a** (global zonal mean of **a**). **c** inhomogeneous part of **a** (**a** minus **b**).

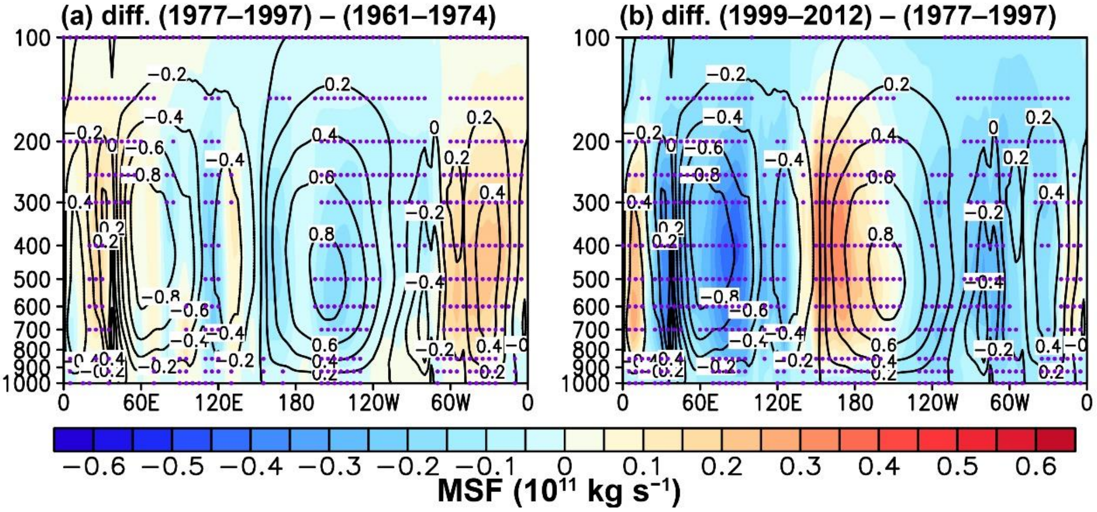

Figure S3 Contours in **a** and **b**: mean state (1961–2012) of the annual mean zonal circulations along the equator (5 °S–5 °N); shading: differences in the annual mean zonal circulations between **a** the periods 1961–1974 and 1977–1997 and **b** the periods 1977–1997 and 1999–2012. The changes statistically significant at the 5% confidence level are dotted in purple. The zonal circulations are represented by the MSF (10^{11} kg s^{-1}) derived from the method developed by Schwendike et al. [1,2].

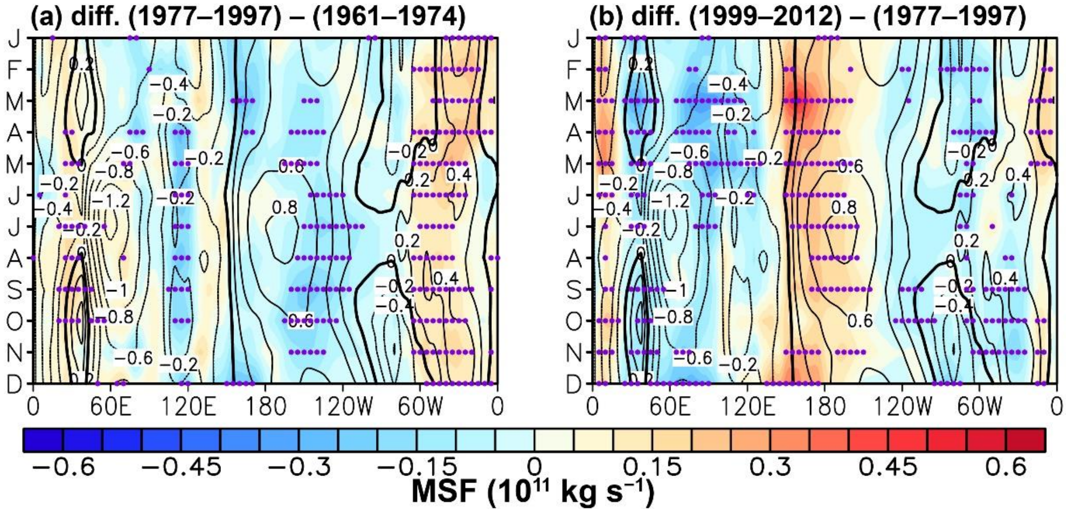

Figure S4 Same as Figure S3 but for the mean state (contours) of and differences (shading) in the monthly mean of vertically averaged zonal circulations. The zonal circulations are represented by the MSF (10^{11} kg s^{-1}) derived from the method developed by Schwendike et al. [1,2].

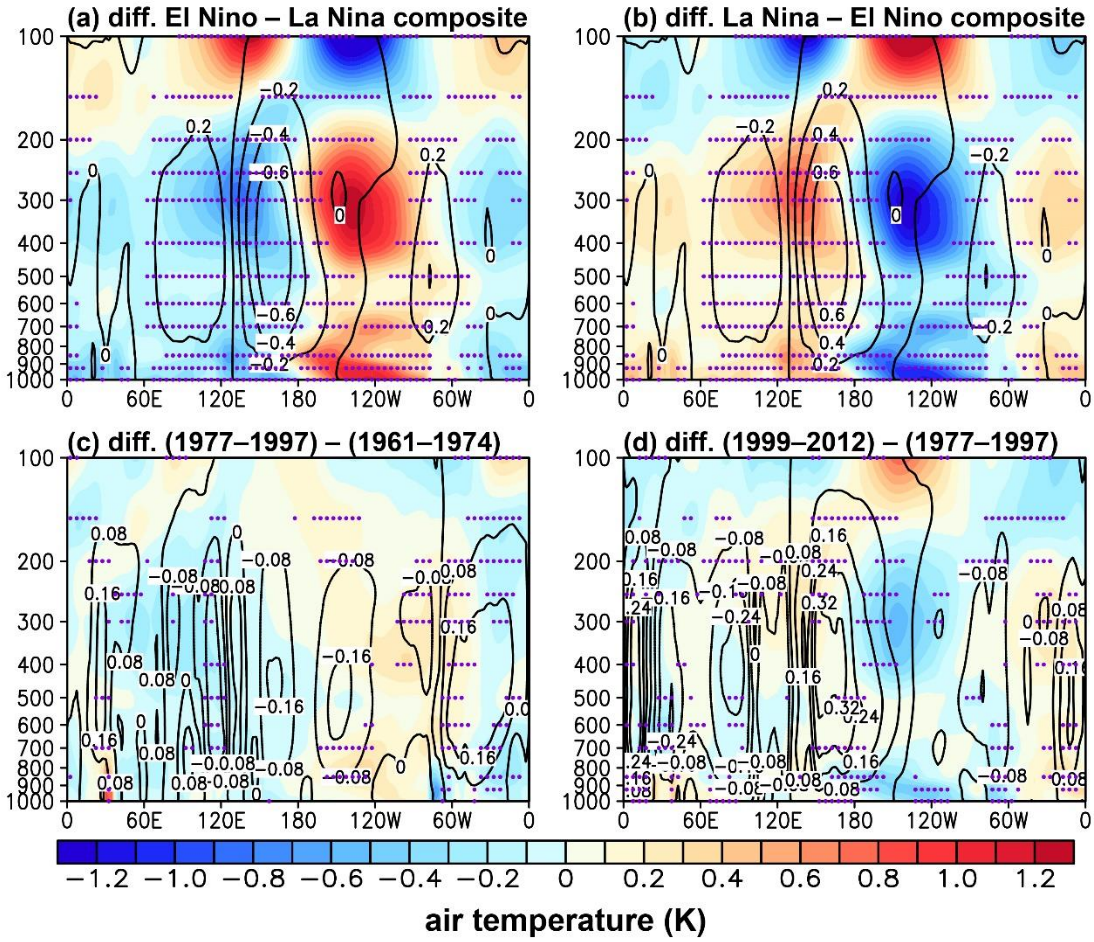

Figure S5 Differences in the zonal circulation (contours; 10^{11} kg s^{-1}) and inhomogeneous air temperature (shading; K) along the equator (5 °S–5 °N) between **a** El Niño and La Niña, **b** La Niña and El Niño, **c** the periods 1961–1974 and 1977–1997, and **d** the periods 1977–1997 and 1999–2012. The zonal circulations are represented by the MSF derived from the method developed by Schwendike et al. [1,2].

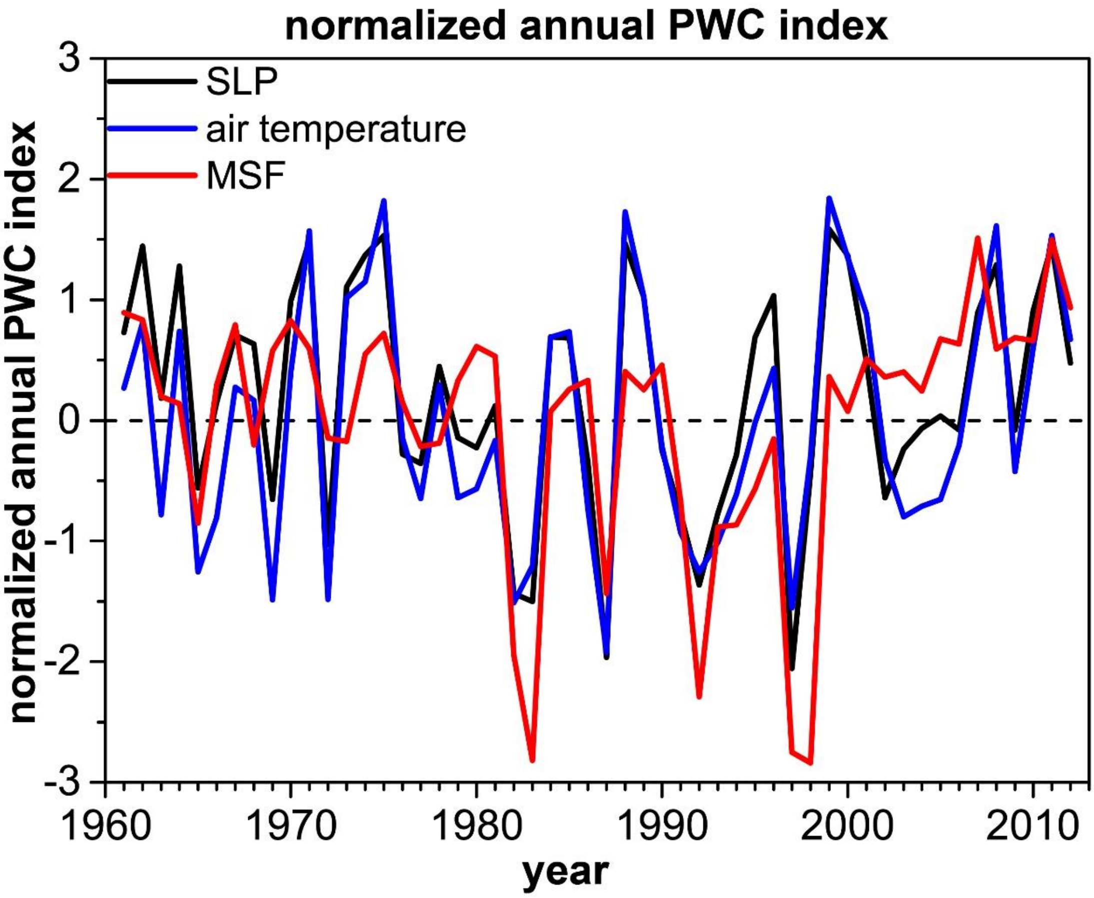

Figure S6 Time series (1961–2012) of the normalized annual mean tropical PWC intensity indices based on the SLP (defined as the mean SLP over the region (5 °S–5 °N, 80 °W–160 °W) minus the mean SLP over the region (5 °S–5 °N, 80 °E–160 °E); black line), air temperature (defined as in Equation (13) in the main text; blue line), and MSF (defined as the mean value of the MSF over the region (5 °S–5 °N, 140 °W–180 °, 300–600 hPa); red line)

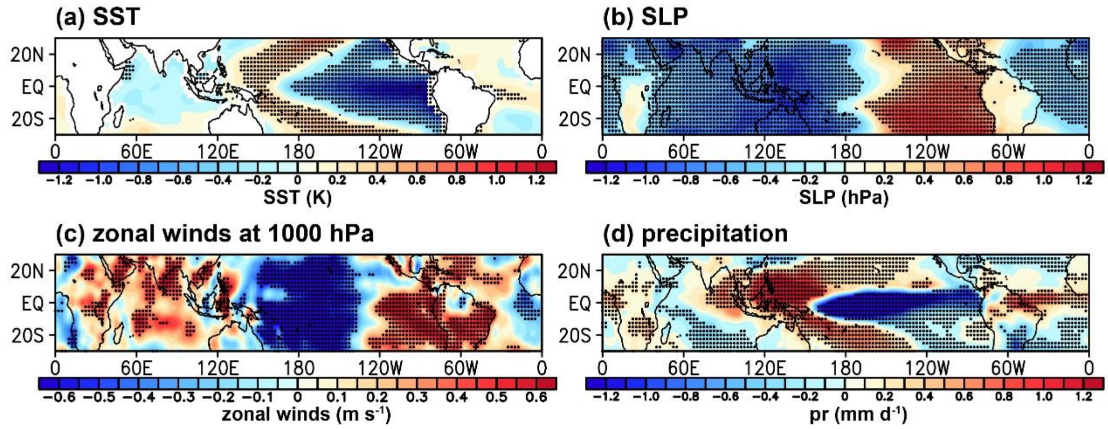

Figure S7 Spatial pattern of the regressed **a** SST (K), **b** SLP (hPa), **c** zonal winds of the zonal circulation at 1000 hPa (m s^{-1}), and **d** precipitation (mm d^{-1}) against the normalized PWC intensity index based on the MSF for the period 1961–2012. The regression coefficients statistically significant at the 5% confidence level are dotted in black.